DOI:
10.1002/adom.201700753

Document Version
Peer reviewed version

Self-assembled silver-germanium nanolayer metamaterial with the enhanced nonlinear response

Tomasz Stefaniuk, Nicolas Olivier, Alessandro Belardini, Cillian P. T. McPolin, Concita Sibilia, Aleksandra A. Wronkowska, Andrzej Wronkowski, Tomasz Szoplik, Anatoly V. Zayats*

Dr. T. Stefaniuk, Dr. N. Olivier, Dr. C. McPolin, Prof. A.V. Zayats
Department of Physics
King's College London
Strand,
London WC2R 2LS, UK
E-mail: tomasz.stefaniuk@kcl.ac.uk

Dr. A. Belardini, Prof. C. Sibilia
Department of Basic and Applied Science for Engineering
Sapienza Università di Roma
Via Antonio Scarpa 16
00161 Roma, Italy

Dr. A. A. Wronkowska, Dr. A. Wronkowski
Institute of Mathematics and Physics
UTP University of Science and Technology
Kaliskiego 7
85-796 Bydgoszcz, Poland

Prof. T. Szoplik
Faculty of Physics
University of Warsaw
Pasteura 7
02-093 Warsaw, Poland

Keywords: Plasmonic metamaterials, second harmonic generation, segregation, silver-germanium composites

Abstract:

Plasmonic metamaterials and metasurfaces are important for many linear and nonlinear photonic applications. Here we show that it is possible to control a nanostructured layer spontaneously formed near an interface of a thin film of silver where the interplay between a grain boundary structure and surface segregation of germanium atoms in silver films leads to encapsulation of the grains and, as a result, formation of a composite metamaterial near the film surface. This Ag/Ge composite exhibits strong localized surface plasmon resonances at

Ge-encapsulated silver grains, leading to extraordinary second harmonic generation for both TM and TE polarized light with up to 2 orders of magnitude enhancement compared to Ag thin films without Ge atoms. Segregation phenomena open the possibility for fabrication of a new class of composite materials and gives additional degree of freedom in designing optical properties of nanostructured metamaterials.

Main Text:

The concept of metamaterials and metasurfaces opened an avenue for designing and fabricating functional optical devices with unique optical properties, relying on geometrical arrangement of nanostructures[1]. Metamaterials have been used to achieve negative refraction[2], controlling density of optical states and spontaneous emission[3, 4], artificial magnetism[5], the enhanced nonlinear properties[6, 7], as well as flat lenses[8, 9] and holograms[10, 11]. In particular the nonlinear properties of plasmonic metamaterials have been intensively exploited. Metals provide some of the highest and fastest nonlinearities compared to semiconducting or transparent dielectrics due to strong local field enhancement, complex electron dynamics and specific designs of the nanostructures which improves the inherent nonlinear optical behavior[12]. Strong Kerr type optical nonlinearity, at the wavelengths where negligible nonlinearity of the constitutive materials exists[7] as well as second- and higher-order harmonic responses were investigated theoretically[13, 14] and experimentally[15, 16]. While it has been proven that metamaterial structure can enhance harmonic generation, the centrosymmetry of metals implies that a break of symmetry such as the one induced by an interface is necessary for generation of even-order harmonics. As the result, only polarization component perpendicular to the surface of metals can efficiently participate in frequency doubling[17, 18] resulting in a strong polarization dependence of second-harmonic generation (SHG), which is dominated under the transverse magnetic (TM)-polarized excitation light

from a smooth surface. While roughness results in relaxation of this rule, overall, the transverse electric (TE)-polarized excitation of SHG is much weaker from centrosymmetric metals.

There are two main approaches for metamaterials fabrication based on top-down nanostructuring and bottom-up self-assembly. The former uses traditional micro- and nano-fabrication methods to form materials from composites of desired shapes and order[8]. In the latter, structuring is achieved by a self-organization process which is controlled by various strategies[19-22]. One of such self-organization processes, called segregation, leads to separation of admixture atoms in small regions within the matrix medium, defined by the presence of inhomogeneities in the matrix, such as free surfaces, grain boundaries, interfaces between different phases or dislocations[23]. Among these, a particularly interesting is segregation at the grain boundaries, which is driven by the reduction of the grain boundary energy. Although its range is limited to the nanometer scale, it can reach much larger concentration differences than other types of segregation[24]. One of the pairs of materials which exhibit segregation is silver and germanium[25]. This combination was rediscovered for plasmonic applications when 1-2 nm thin germanium (Ge) wetting films were proposed to overcome silver (Ag) tendency to form clusters rather than smooth layers[26-28]. However, it has been recently shown that the penetration of Ge atoms along high-diffusivity paths in silver not only changes the resistivity of silver thin films[29], but also has a significant impact on their optical properties[30].

In this paper, we use the segregation mechanism to form Ag/Ge nanolayer metamaterial with unique nonlinear optical properties. We show that apart from the localized surface plasmon (LSP) resonances exited due to surface roughness, this system exhibits LSPs originating from Ge-encapsulated silver grains, which have strong influence on the optical properties of the thin Ag/Ge films. The segregation process breaks the centrosymmetry of silver host, leading

to generation of SH for TM- and, extraordinary, for TE-polarized excitation light with up to 2 orders of magnitude enhancement compared to smooth Ag films without Ge.

The Ag/Ge nanolayer metamaterial (Figure 1b and S1) was formed by Ge diffusion and segregation near the Ag-air interface (see Experimental section for the details of fabrication). The presence of the 1 nm amorphous Ge wetting layer during the e-beam evaporation process of Ag changes the kinetics of growth of Ag and smoothens even a 100 nm thick silver film. The average diffusion length of Ag adatoms is significantly shorter on Ge than on SiO_2 substrate, resulting in a more compact silver film with smaller grain sizes[31, 32]. The Ag/Ge sample has a more uniform distribution of nanocrystals at the surface and lacks large crystallites, compared to Ag film (Figure 1a).

The small variation of reflectance observed for a pure Ag film near a wavelength of 360 nm (Figure 1c) can be associated with LSP excitations due to the roughness of the film[30]. They disappear for a smoother Ag/Ge metamaterial. The reflection spectra of the Ag/Ge nanonalayer metamaterial reveal a strong absorption resonance at around 640 nm wavelength, absent in Ag film without Ge, whose origin can be traced to LSPs of Ge-encapsulated silver grains. This peak increases with time together with DC resistivity[29] and can be attributed to segregation of Ge atoms from the wetting layer towards the surface of Ag film, as observed in *ex-situ* X-ray photoelectron spectroscopy measurements[30]. This process evolves in time and 14 days after the evaporation, only a fraction of the original amount of Ge atoms remains on Ag-substrate interface[30] while most of the Ge atoms segregate to the Ag film free interface, which can be considered as largest defect in the structure, and into silver grain boundaries near the Ag-air interface. For comparison, when a 1 nm thick Ge layer is evaporated on top of a pure silver, the reflection spectrum no longer exhibits the resonance related to the encapsulation of the silver grains in Ag/Ge composite. Since the film surface has the lowest Gibbs energy, Ge atoms no longer have a tendency to segregate inside the Ag film and to

form a composite. Classical diffusion process however is not blocked. If a Ag/Ge metamaterial is additionally covered with a 10 nm thick layer of amorphous SiO_2, the features of the reflection spectrum related to LSPs due to both the roughness and encapsulated Ag/Ge grains can still be observed. The latter one is however suppressed since the presence of fused silica limits the segregation of Ge to the SiO_2/Ag interface as the surface states are already occupied by SiO_2 atoms. Silica layer also leads to a shift of both LSP resonances due to the changes of refractive indexes of the adjacent medium, as expected for LSP modes (see Supporting Information for more details). The position of the resonances can be also controlled by changing the size of the silver grains. Different sizes can be obtained by, e.g., varying the substrate temperature during the evaporation process[28], altering the amount of Ge atoms [32] or modifying the thickness of the Ag film. The measured spectra of the imaginary part of the effective permittivity of the Ag/Ge composite obtained with the Ag films of different thicknesses 100 nm, 20 nm and 10 nm show that similarly to the plasmonic nanoparticles of decreasing diameter, thinner films and, thus, smaller grain diameters lead to the shift of the LSP mode towards shorter wavelengths (Figure 1e).

The optical properties of the Ag/Ge grain composite near the surface of the film were modelled assuming that in equilibrium the silver grains are encapsulated by Ge atoms that breaks the electrical connection between the grains. This may occur if at the beginning the Ge atoms segregate to low-coordination-number surface states and only when they are occupied they stay in high-coordination-number Ag grain boundary states. The simulated reflection spectra of Ag/Ge nanolayer metamaterial (Figure 1d, blue and red line) and the corresponding intensity distributions (Figure 2a and 2b) well describe the experimental data for both rough Ag films and smooth Ag/Ge composites. The pure Ag film, modelled with grains of 30 nm size near the interface with air, exhibits a LSP at 356 nm wavelength and the incident electromagnetic field is concentrated near the surface of the film. In the case of Ag/Ge

metamaterial, the absorption maximum is near a wavelength of 640 nm corresponding to the LSP on the Ge-encapsulated, isolated silver grains of 20 nm size. In this situation, the field is strongly concentrated below the surface around the grains. The metal between the grains of the composite, prevents electromagnetic interaction between them and, thus, the optical properties are determined by the behavior of individual grains. For the 2 other geometries considered in the experiment, with Ge on top of a Ag film and with a silica protective layer (Figure 1d, black and green lines, respectively), the numerical model confirms that without the presence of germanium at the boundary sites, the LSP resonance indeed does not exist, while a silica layer shifts the LSPs of the Ag/Ge composite due to its refractive index, as long as the amount of Ge atoms between the grains is enough to sever the electrical connection.

The grain structure of the composite near the Ag-air interface and the associated resonant field enhancement (Figure 2) have profound impact also on the nonlinear optical properties (Figure 3 and S3). The observed SHG from the Ag film (solid lines) is much stronger under excitation with TM-polarized light, which should be expected for relatively smooth continuous metal surfaces[33] (see Figure S3). Only the component of the electric field normal to the metal surface has a discontinuity at the boundary and gives rise to a dipole-allowed surface nonlinearity[34]. The decrease in the SH intensity near the interband transitions (around a wavelength of 310 nm) is also expected and results from the interplay between free-electron plasma and core electrons in metals[35].

The second-harmonic spectra from the Ag/Ge nanolayer metamaterial are significantly different (Figure 3a and 3b). Although, the presence of Ge atoms introduces extra losses, and, thus, the nonresonant SH signal is weaker, near the LSP resonance excited on the encapsulated grains, the situation dramatically changes. For TM-polarized light, the generated SH signal at a wavelength of 325 nm is almost 20 times stronger than from the Ag surface under the same illumination conditions and, despite the vicinity of the interband transitions,

the intensity is almost 40% stronger than the highest SH intensity in all the measured spectral range (Figure 3c). Surprisingly, the SH signal enhancement is also observed for the TE-polarized light in the same spectral range. Not only does the enhancement factor at the LSP resonance exceeds 300, but the SH intensity is now of the same order of magnitude as the intensity observed under TM-polarized illumination in metamaterial and much stronger than from a pure Ag surface. The wavelength dependence of SH intensity enhancement follows the behavior of the imaginary part of the effective permittivity of Ag/Ge (Figure 3d).

SHG is a second-order nonlinear process and its intensity is proportional to the square of the fundamental light intensity. Therefore, different efficiencies of the SH generation in the metamaterial for TM- and TE-polarized light compared to a Ag surface can be explained in terms of the LSP field enhancement near the surface of a film, which is 2 times stronger for the TM polarization (Figure 2c and 2d), and symmetry breaking introduced by the encapsulated Ag grains (Figure S3). The grain encapsulation increases the effective surface area needed for second-order nonlinear response. As the result, not only does the component of the electric field normal to the smooth air-metal interface (E_z) participate in the frequency doubling, but so do the other components (E_x and E_y), which are usually not active in SHG process at metal interface, as they now, efficiently generate SH light from the grain boundaries below the air-metal interface. In practice it means that it is possible to obtain strong SH signal and smooth film surface at the same time.

We have demonstrated that the segregation mechanism leads to the formation of a nanolayer metamaterial which exhibits enhanced and polarization independent SHG. This unique process breaks nonlinear optics paradigms of polarization selection rules of a dipole-allowed surface nonlinearity in centrosymmetric media. The spontaneously formed encapsulated grains near the surface determine both the polarization and wavelength dependent SH efficiency via their localized surface plasmon resonances. We show that strong frequency

doubling can be achieved even at wavelengths where the interband transitions significantly reduce the nonlinear response of the metal, with up to 2 orders of magnitude enhancement compared to a rough Ag film. These results demonstrate the potential of a new class of composite metamaterials which can be formed using segregation processes and can be achieved in many plasmonic metals[24]. Bottom-up segregation process together with additional top-down nanostructuring may lead to 2-level hierarchical metamaterials and nanolayer metamaterial with the extended range of linear and nonlinear functionalities which are difficult to achieve in conventional metamaterials due to constituent material constraints.

Experimental section

Sample fabrication and physical characterization: Thin films were deposited using an electron-beam evaporator (PVD75, Lesker). During the evaporation process, the pressure in the chamber was 2×10^{-6} Torr and the sample holder was kept at room temperature. Double-sided polished fused silica glass substrates with nominal roughness RMS $\leq$ 0.3 nm (root mean square), were cleaned for 30 s with argon ions having 105 eV energy and a 0.2 mA/ cm^2 beam density before the deposition of layers. Ge films of 1 nm thickness were evaporated at the rate of 0.5 Å/s, Ag layers of 100 nm thickness at the rate of 10 Å/s and 10 nm thick SiO_2 overlayer at the rate of 1 Å/s. Subsequent layers were sequentially evaporated without breaking the vacuum. Film thicknesses were monitored using the oscillating quartz crystal. Atomic force microscope (AFM Ntegra NT-MDT) measurements under tapping mode in air were carried to estimate the quality of the evaporated surfaces. Before characterization, the samples were kept in ambient conditions in an Ar atmosphere. The averaged RMS values from AFM scans are 1.8±0.3 for Ag/Ge samples and 3.74±0.4 nm for Ag films. The scanning electron microscopy (SEM) images of the samples were taken using the Zeiss Sigma microscope with acceleration voltage of 20 kV (Figure 1a and b). The grain boundaries are not necessarily clearly visible in SEM or AFM images, since both measurements characterize only the film surface. Therefore,

the interior structure of samples was investigated using one-dimensional, wide-angle X-ray diffraction (Bruker GADDS system equipped with 2D Vantec 2000 detector). Under the assumption that a Ag layer consists of crystallites with some average size τ, its value can be estimated via the Debye−Scherer equation $\tau=0.89\lambda/(\beta \cos \theta)$, where λ is the X-ray wavelength (1.5406 Å), θ is the Bragg diffraction angle, and β is the line broadening at the half maximum. On the basis of spectra presented in Figure S4, the averaged grain size of the Ag/Ge metamaterial estimated to be approximately 20 nm and used in numerical simulations. The skin-depth of Ag is 12 nm at around 640 nm wavelength which is comparable to the size of the encapsulated grains. The grain size of the pure Ag reference film varies between 30 nm and 50 nm, depending on a particular area of the sample.

Linear optical characterization: Reflectance (Figure 1c) and ellipsometry (Figure 2d) measurements were performed in air using a rotating analyzer ellipsometer in the spectral range from 300 to 1000 nm (V-VASE, J.A. Woollam Co., Inc.). Ellipsometric parameters Ψ and Δ were determined for angles of incidence in the range $40° \leq \varphi \leq 80°$. Optical constants of the samples were calculated from the measured quantities using a regression procedure and the parametrization of optical functions model to match the experimental data. For the same fabrication conditions and same film thickness, the position of the resonance for different samples varies only by ± 20nm, and most of this fluctuation is due to the time evolution of the segregation process.

Nonlinear spectroscopy: An amplified Yb:KGW femtosecond laser (Pharos, Light Conversion) together with an optical parametric amplifier (Orpheus, Light Conversion) were used to achieve light pulses in the wavelength range of 650-850 nm. 150 fs pulses with 100 kHz repetition rate were sent through a range of optical components (Figure S2) to control of polarization, power, divergence, and size of the beam. The peak power focused at the sample surface using an Olympus LMPLN10XIR objective was of the order of 70 GW/cm^2 and the

sample position was adjusted for every illumination wavelength. The residues of the fundamental incident beam were filtered out using band-pass filters (Thorlabs). The SH spectra were collected using a spectrometer (IsoPlane SCT320, Princeton Instruments) equipped with a UV camera (ProEM:eXcelon3, Princeton Instruments) and were corrected to the transmission properties of the filters and objectives in the setup. The enhancement factor is defined as a ratio between SH signal intensity measured for Ag/Ge nanolayer metamaterial and pure Ag reference sample (Figure 3). The nonlinear optical characterization was performed 4 months after the evaporation of the samples.

Numerical modelling: To understand the nature of the metamaterial resonance, a Finite Difference Time Domain modelling (Lumerical FDTD solutions) of the structure was performed taking into account the internal grain structure of the Ag/Ge film. We assumed that at the beginning the Ge atoms segregate to low-coordination surface states and only when they are occupied they stay in high-coordination Ag grain boundary states. As a result, in the equilibrium the silver grains are being encapsulated by Ge-type thin layer which breaks the electrical connection between the grains[29]. On the basis of these hypothesis, we retrieved reflection curves (Figure 1d) and the corresponding field intensity distributions (Figure 3a and 3b). The sizes of the grains are estimated on the basis of X-ray diffraction measurements and are chosen as 20 nm for Ag/Ge composite and 30 nm for Ag reference sample. The center to center separation of the grains are chosen as 45 nm. The effective refractive index of the Ge nanoshell is $n_{Ag/Ge}$=1.1+0.1i and a 1.5 nm shell thickness is assumed. Although we use a relatively simple model to describe the complex geometrical structure of the composite material, the simulations for both the pure silver film and the metamaterial provide good agreement with the measured data. The estimated shell refractive index is between the refractive index of 100 nm thick Ag reference sample (n_{Ag}=0.064+4.285i) and 1 nm thick amorphous layer of germanium (n_{Ge}=3.33+0.24i), measured for 645 nm wavelength in our

experiments. The refractive index of SiO_2 cover layer equals $n_{SiO2}=1.462 + 0i$ for the same frequency.

Acknowledgements
This work has been supported, in part, by EPSRC (UK) and the ERC iPLASMM project (321268). A.Z. acknowledges support from the Royal Society and the Wolfson Foundation.

REFERENCES

[1] R. A. Shelby, D. R. Smith, S. Schultz, *Science* **2001**, 292, 77.

[2] C. M. Soukoulis, S. Linden, M. Wegener, *Science* **2007**, 315, 47.

[3] M. A. Noginov, H. Li, Y. A. Barnakov, D. Dryden, G. Nataraj, G. Zhu, C. E. Bonner, M. Mayy, Z. Jacob, E. E. Narimanov, *Opt. Lett.* **2010**, 35, 1863.

[4] J. Li, A. V. Krasavin, L. Webster, P. Segovia, A. V. Zayats, D. Richards, *Sci. Rep.* **2016**, 6, 21349.

[5] T. J. Yen, W. J. Padilla, N. Fang, D. C. Vier, D. R. Smith, J. B. Pendry, D. N. Basov, X. Zhang, *Science* **2004**, 303, 1494.

[6] G. A. Wurtz, R. Pollard, W. Hendren, G. P. Wiederrecht, D. J. Gosztola, V. A. Podolskiy, A. V. Zayats, *Nat. Nanotechnol.* **2011**, 6, 107.

[7] A. D. Neira, N. Olivier, M. E. Nasir, W. Dickson, G. A. Wurtz, A. V. Zayats, *Nat. Commun.* **2015**, 6, 7757.

[8] N. Yu, F. Capasso, *Nat. Mater.* **2014**, 13, 139.

[9] A. V. Kildishev, A. Boltasseva, V. M. Shalaev, *Science* **2013**, 339, 12320091.

[10] X. Ni, A. V. Kildishev, V. M. Shalaev, *Nat. Commun.* **2013**, 4, 2807.

[11] W. T. Chen, K. Y. Yang, C. M. Wang, Y. W. Huang, G. Sun, I. D. Chiang, C. Y. Liao, W. L. Hsu, H. T. Lin, S. Sun, L. Zhou, A. Q. Liu, D. P. Tsai, *Nano Lett.* **2014**, 14, 225.

[12] M. Kauranen, A. V. Zayats, *Nat. Photonics* **2012**, 6, 737.

[13] M. Scalora, M. A. Vincenti, D. de Ceglia, V. Roppo, M. Centini, N. Akozbek, M. J. Bloemer, *Phys. Rev. A* **2010**, 82, 043828.

[14] P. Ginzburg, A. V. Krasavin, G. A. Wurtz, A. V. Zayats, *ACS Photonics* **2015**, 2, 8.

[15] M. W. Klein, C. Enkrich, M. Wegener, S. Linden, *Science* **2006**, 313, 502.

[16] A. Belardini, M. C. Larciprete, M. Centini, E. Fazio, C. Sibilia, D. Chiappe, C. Martella, A. Toma, M. Giordano, F. Buatier De Mongeot, *Phys. Rev. Lett.* **2011**, 107, 257401.

[17] J. E. Sipe, V. C. Y. So, M. Fukui, G. I. Stegeman, *Phys. Rev. B* **1980**, 21, 4389.

[18] C. Forestiere, A. Capretti, G. Miano, *J. Opt. Soc. Am. B* **2013**, 30, 2355.

[19] K. Sadecka, J. Toudert, H. B. Surma, D. A. Pawlak, *Opt. Express* **2015**, 23, 19098.

[20] M. Xiong, X. Jin, J. Ye, *Nanoscale* **2016**, 8, 4991.

[21] V. A. Turek, Y. Francescato, P. Cadinu, C. R. Crick, L. Elliott, Y. Chen, V. Urland, A. P. Ivanov, L. Velleman, M. Hong, R. Vilar, S. A. Maier, V. Giannini, J. B. Edel, *ACS Photonics* **2016**, 3, 35.

[22] M. E. Nasir, S. Peruch, N. Vasilantonakis, W. P. Wardley, W. Dickson, G. A. Wurtz, A. V. Zayats, *Appl. Phys. Lett.* **2015**, 107, 121110.

[23] H. Mehrer, *Diffusion in Solids: Fundamentals, Methods, Materials, Diffusion-controlled Processes*, Springer-Verlag Berlin and Heidelberg GmbH & Co. KG, Berlin, Germany **2009**.

[24] P. Lejcek, *Grain Boundary Segregation in Metals*, Springer Publishing Company, Incorporated, Berlin, Germany, **2010**.

[25] A. L. Wachs, T. Miller, T. C. Chiang, *Phys. Rev. B* **1986**, 33, 8870.

[26] V. J. Logeeswaran, N. P. Kobayashi, M. S. Islam, W. Wu, P. Chaturvedi, N. X. Fang, S. Y. Wang, R. S. Williams, *Nano Lett.* **2009**, 9, 178.

[27] W. Chen, M. D. Thoreson, S. Ishii, A. V. Kildishev, V. M. Shalaev, *Opt. Express* **2010**, 18, 5124.

[28] T. Stefaniuk, P. Wróbel, E. Górecka, T. Szoplik, *Nanoscale Res. Lett.* **2014**, 9, 1.

[29] T. Stefaniuk, P. Wróbel, P. Trautman, T. Szoplik, *Appl. Opt.* **2014**, 53, B237.

[30] P. Wróbel, T. Stefaniuk, M. Trzcinski, A. A. Wronkowska, A. Wronkowski, T. Szoplik, *ACS Appl. Mater. Interfaces* **2015**, 7, 8999.

[31] D. Flötotto, Z. M. Wang, L. P. H. Jeurgens, E. Bischoff, E. J. Mittemeijer, *J. Appl. Phys.* **2012**, 112, 043503.

[32] J. Zhang, D. M. Fryauf, M. Garrett, V. J. Logeeswaran, A. Sawabe, M. S. Islam, N. P. Kobayashi, *Langmuir* **2015**, 31, 7852.

[33] K. A. O'Donnell, R. Torre, C. S. West, *Phys. Rev. B* **1997**, 55, 7985.

[34] F. Brown, R. E. Parks, A. M. Sleeper, *Phys. Rev. Lett.* **1965**, 14, 1029.

[35] N. Bloembergen, R. K. Chang, C. H. Lee, *Phys. Rev. Lett.* **1966**, 16, 986.

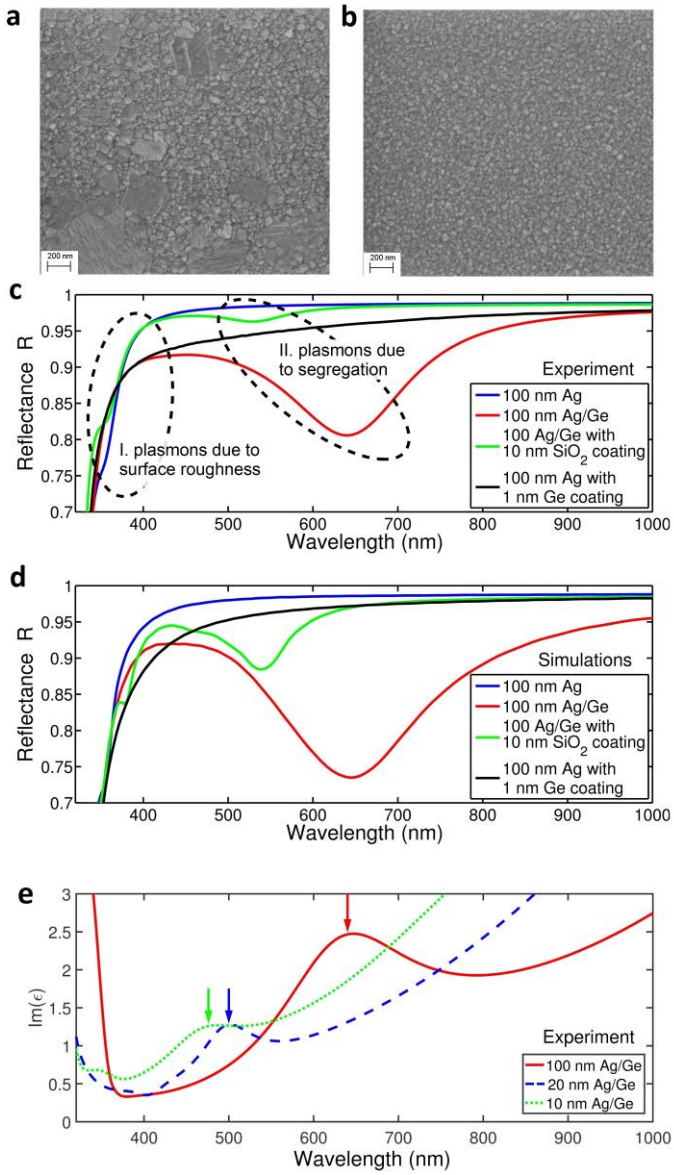

Figure 1. Linear optical properties of Ag/Ge nanolayer metamaterial. SEM images of (a) Ag reference film and (b) Ag/Ge metamaterial. (c) Experimentally measured and (d) numerically simulated reflectance spectra at normal incidence for different surface types. (e) Spectra of the imaginary part of the effective permittivity of the Ag/Ge nanolayer metamaterial obtained for Ag films of different thicknesses and the same thickness of Ge layer (1 nm). The samples parameters are shown in the legend in panels c-e.

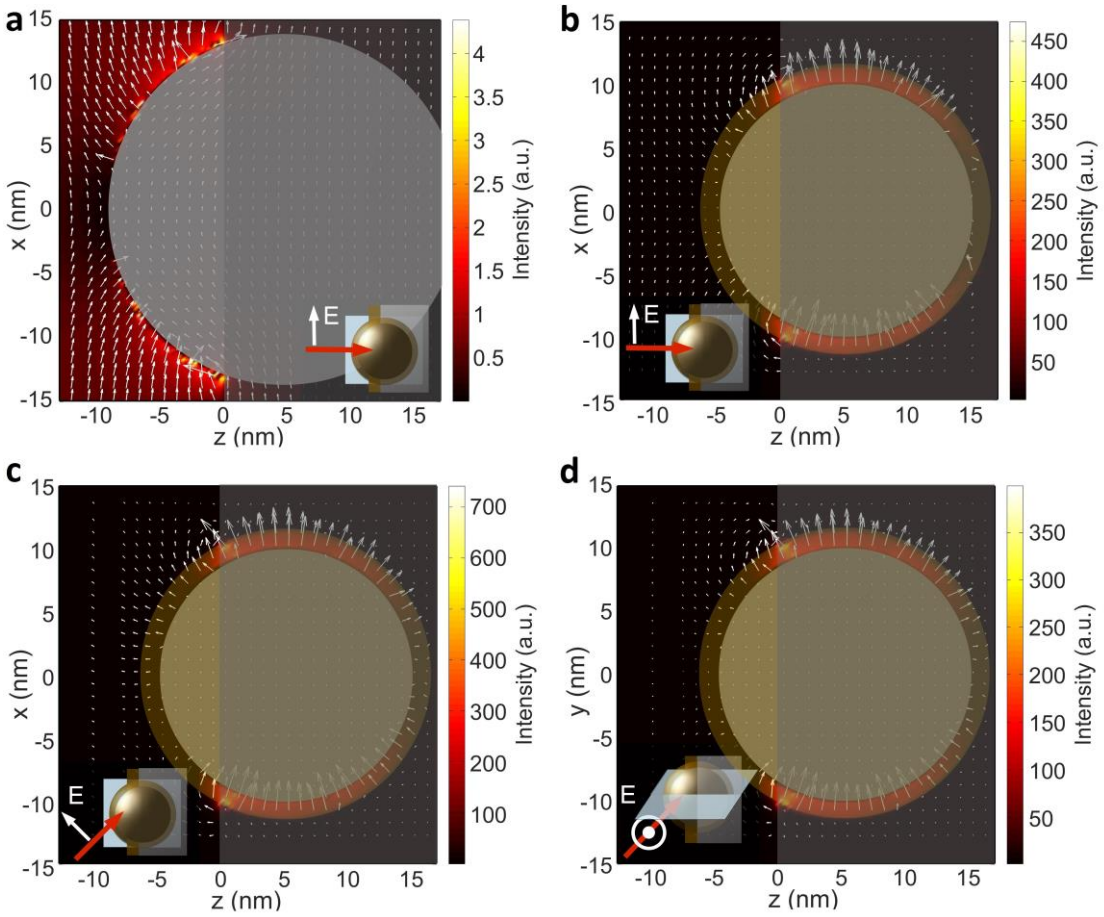

Figure 2. FDTD simulation of the LSP-induced intensity distributions in the nanolayer metamaterial. Intensity (colour maps) and direction of the electric field (arrows) around the silver grains in (a) pure silver layer (30 nm grains) and (b-d) Ge-encapsulated Ag grains (20 nm) at a wavelength of 640 nm under (a, b) normal incidence and (c) TM-polarized and (d) TE-polarized illumination at 45° incidence. z=0 corresponds to surface level. Gray circles represent Ag grains. Brown circles depict Ge encapsulation of silver grains. Dark gray slab represents the Ag film volume. The insets show the orientation of the presented cross-sections.

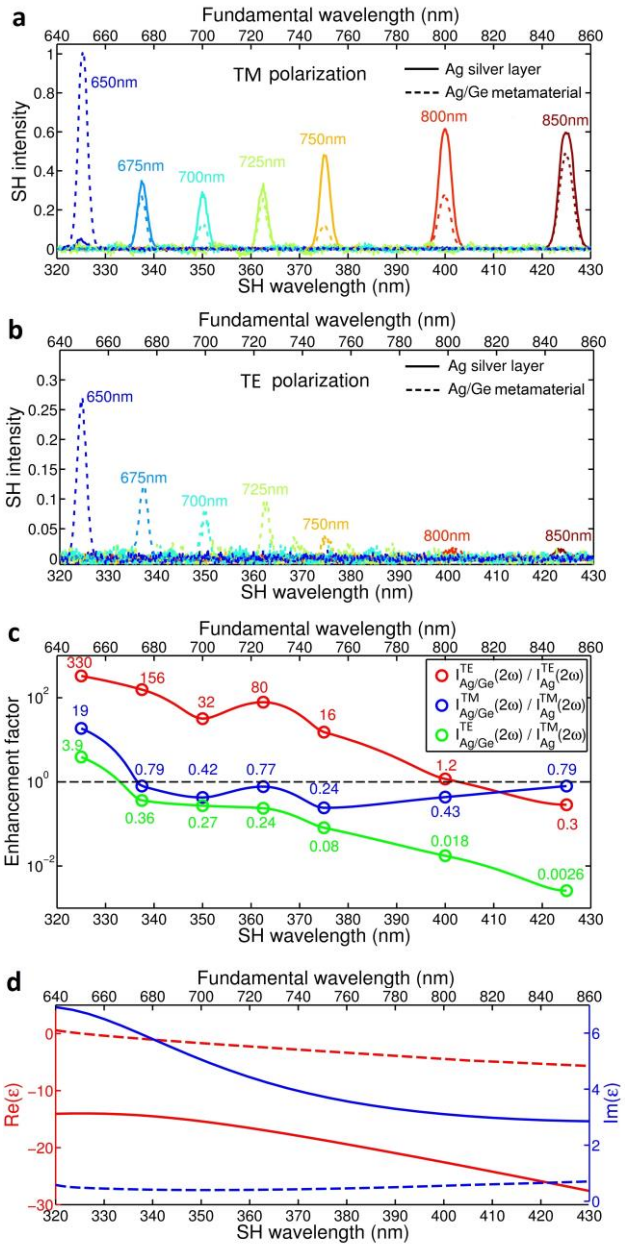

Figure 3. Nonlinear properties of Ag/Ge nanolayer metamaterial. Intensity of SH signal generated from Ag surface (solid lines) and Ag/Ge metamaterial (dashed lines) for (a) TM-polarized and (b) TE-polarized incident light for different fundamental wavelengths. (c) Spectra of the SHG enhancement factor for different fundamental light polarizations. (d) Spectra of the real (red lines) and imaginary (blue lines) part of the effective permittivity of the Ag/Ge metamaterial measured in 640-860 nm (solid lines) and 320-430 nm (dashed lines) wavelength ranges, corresponding to the studied fundamental and SH wavelengths.

The table of contents

We demonstrate fabrication of a new class of composite plasmonic materials with unique nonlinear optical properties. We show that due to segregation process, spontaneously formed smooth Ag/Ge nanolayer metamaterial exhibits strong localized surface plasmon resonances leading to extraordinary second harmonic generation for both TM and TE polarized light with up to 2 orders of magnitude enhancement.

Keyword

Plasmonic metamaterial

Tomasz Stefaniuk*, Nicolas Olivier, Alessandro Belardini, Cillian McPolin, Concita Sibilia, Aleksandra A. Wronkowska, Andrzej Wronkowski, Tomasz Szoplik, Anatoly V. Zayats

Title

Self-assembled silver-germanium nanolayer metamaterial with the enhanced nonlinear response

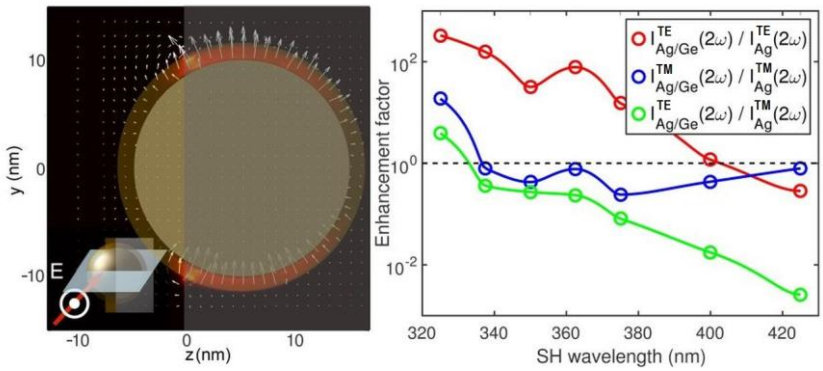

Supporting Information

Title Self-assembled silver-germanium nanolayer metamaterial with the enhanced nonlinear response

Tomasz Stefaniuk, Nicolas Olivier, Alessandro Belardini, Cillian McPolin, Concita Sibilia, Aleksandra A. Wronkowska, Andrzej Wronkowski, Tomasz Szoplik, Anatoly V. Zayats*

Segregation is a faster process than diffusion at temperatures lower than 0.6 of meting temperature of the matrix, which is approximately 1000 K in the case of a 100 nm thick Ag film[1], thus the optical properties of the nanolayer metamaterial evolve at ambient conditions. With the increasing amount of Ge atoms near the air-Ag interface the refractive index of the shell around the grains increases and the surface resistivity rises. (In the manuscript, the term "grains" does not refer to clusters or islands of silver but to 2D defects in the silver crystal structure and, therefore, there can be can be several silver grains in the volume of one silver cluster.)This leads to the shift of LSP resonance exited at the encapsulated grains towards longer wavelengths with time after the film evaporation. The evaporation of fused silica overlayer changes the segregation dynamic. The lack of Ge atoms at the surface causes blue shift of the resonance and, thus, the dip in the reflection spectra since the SiO_2 refractive index is lower than amorphous Ge thin layer (Figure 1c and 1d). The LSP resonance related to sample roughness is still visible in the spectrum and shifted towards longer wavelengths with the respect to the resonances of the uncoated Ag film.

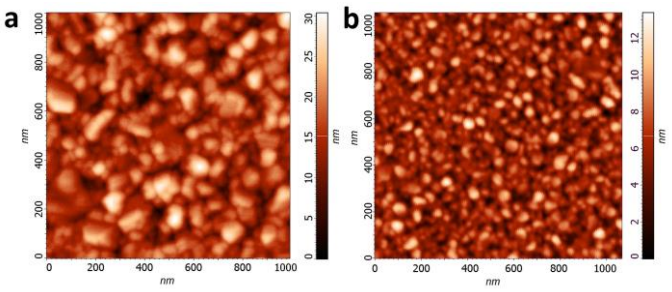

Figure S1. AFM images of (a) Ag reference film and (b) Ag/Ge nanolayer metamaterial. The averaged RMS values are 3.74±0.4 nm for Ag films and 1.8±0.3 for Ag/Ge samples.

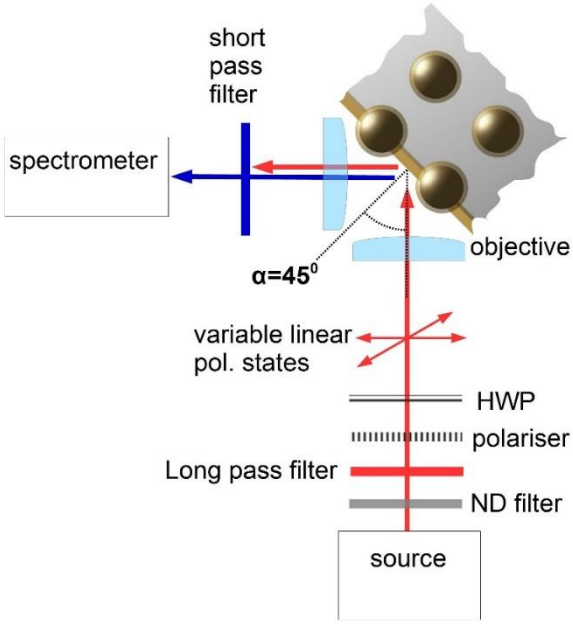

Figure S2. Schematic of the SHG measurements.

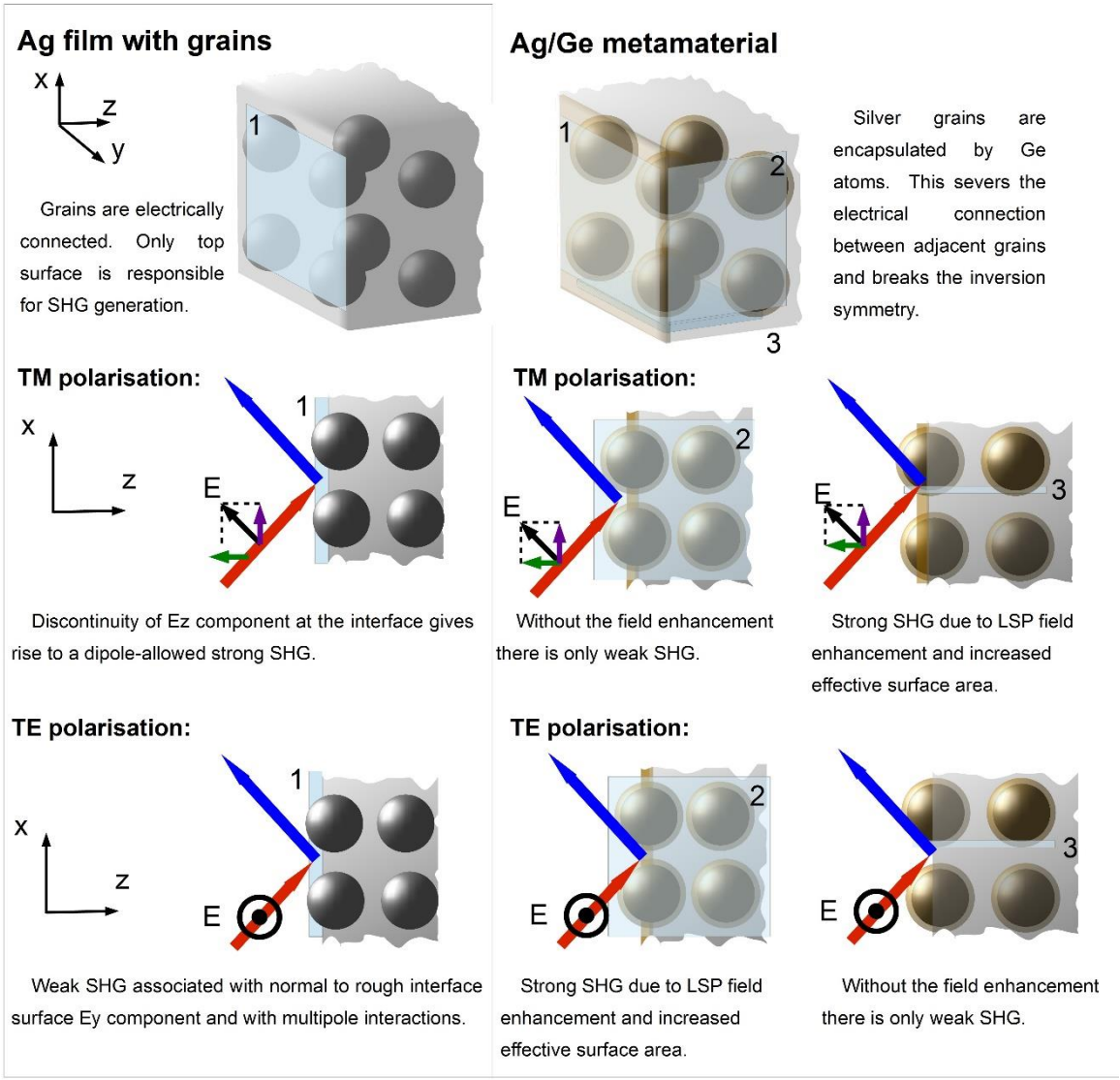

Figure S3. Schematics of nonlinear light interaction with a rough Ag film and Ag/Ge nanolayer metamaterial. Spheres represent grains of the Ag film near the surface: (black) electrically connected and (brown) electrically disconnected. (Red) fundamental light and (blue) SH light.

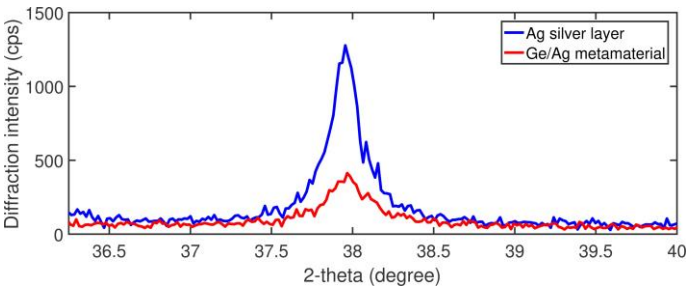

Figure S4. One dimensional X-ray diffraction of 100 nm thick silver layer and 100 nm thick Ag/Ge nanolayer metamaterial. The sample with Ge atoms exhibits broader (111) peak which manifests smaller grains.

[1] H. Mehrer, *Diffusion in Solids: Fundamentals, Methods, Materials, Diffusion-controlled Processes*, Springer-Verlag Berlin and Heidelberg GmbH & Co. KG, Berlin, Germany **2009**.